X Encontro Brasileiro sobre Adsorção
27 a 30 de Abril de 2014
Guarujá - SP

CARBON DIOXIDE ADSORPTION USING ORGANOFUNCTIONALIZED MAGNESIUM PHYLLOSILICATES AS ADSORBENTS BY TERMOPROGRAMED DESORPTION

K. O. Moura[1]; H. O. Pastore[1*]

1-Grupo de Peneiras Moleculares Micro- e Mesoporosas, Instituto de Química, Universidade Estadual de Campinas (UNICAMP), Rua Monteiro Lobato, 270. CEP: 13083-861 – Campinas – São Paulo, Brazil. Telefone: (19) 35213017 – Email: gpmmm@iqm.unicamp.br

ABSTRACT: Carbon dioxide adsorbents, constituted by organofunctionalized magnesium phyllosilicates, were produced using 3-aminopropyltriethoxysilane (N1), N-[3-(trimethoxysilyl)propyl]-ethylenediamine (N2), N-[3-(trimethoxysilyl)propyl]-diethylenetriamine (N3) and tetraethoxyorthosilane (TEOS) as silicon sources with N/Si ratios of 1, 0.75, 0.5 and 0.25, by conventional and microwave heating. Adsorption studies were performed using temperature programmed desorption (TPD) methods. The results showed that the maximum adsorption capacity was between 0.67 and 3.64 mmol g^{-1}, for 8.33% N3 by microwave and 33.33% N3 by conventional heating, respectively, with maximum efficiency from 0.28 to 0.90 for 100% N1 and 33.33% N3, obtained by conventional heating. Desorption kinetics of CO_2, described using Avrami's model, show that the CO_2 desorption rate constant is in the range from 0.13 to 0.18 min^{-1}, similar to the values for CO_2 desorption from monoetamolamine-functionalized TiO_2 and Li_4SiO_4 but in a narrower range of values.

KEYWORDS: carbon dioxide; desorption; magnesium phyllosilicate.

1. INTRODUCTION

Carbon dioxide has been considered the most important greenhouse gas; its rate of increase in the atmosphere progressed from less than 1 ppm $year^{-1}$ before to 1970 to more than 2 ppm $year^{-1}$ in the last years (Sayari *et al.*, 2011).

Adsorption on solids has been considered a potential option for CO_2 capture, due to the low energy consumption involved, the cost advantages of the process and the ease of use on a wide range of temperatures and pressures (Shafeeyan *et al.*, 2010). The use of the appropriated adsorbents can potentially decrease the cost associated with the CO_2 uptake in capture and storage technology. Organic-inorganic hybrid materials as CO_2 adsorbent have emerged as a process close to application.

According to the literature, several types of supported alkylamines have been used as CO_2 adsorbent (Samanta *et al.*, 2012). Usually, the most used solid supports are mesoporous silica, such as MCM-41, MCM-48, SBA-15 and SBA-16 (Sayari *et al.*, 2011); zeolites (Jadhav *et al.*, 2007); active carbon (Plaza *et al.*, 2007); and layered solids, like LDH (Wang *et al.*, 2012), ITQ-6 (Zukal *et al.*, 2009) and montmorillonite (Stevens *et al.*, 2013). Since that layered materials allow a high contact area between adsorption sites and CO_2, the use of supported amines in layered solids for CO_2 capture has been investigated in our research group using polyethylenimine (Vieira and Pastore, 2014) and 3-aminopropyltriethoxysilane (N1) (Moura and Pastore, 2014) on magadiite, and N1, N-[3-(trimethoxysilyl)propyl]-ethylenediamine (N2), N-[3-(trimethoxysilyl)propyl]-

diethylenetriamine (N3) on magnesium phyllosilicates (Moura and Pastore, 2013).

Recently, we reported the direct synthesis of organo-functionalized magnesium phyllosilicate under conventional (Ferreira *et al*., 2008) and microwave (Moura and Pastore, 2014) synthesis conditions. The syntheses of these materials using several different organosiloxanes and their application in catalysis (Patel *et al.*, 2008) antimicrobial activity (Chandrasekaran *et al.*, 2011) and adsorption of metals (Lagadic *et al.*, 2001) and dyes (Lee *et al*., 2011) have been studied.

In the present work, organo-functionalized magnesium phyllosilicate obtained by direct synthesis, using N1, N2, N3 and tetraethoxyorthosilane (TEOS) as silicon sources, in several molar proportions of the amines relative to total silicon, and conventional or microwave heating, will be used as carbon dioxide adsorbents. Factors such as molar proportions of the amines presented in the solid, and heating type used in the synthesis of the solids will be discussed here. Kinetic study using Avrami's model was also perform.

2. EXPERIMENTAL PART

2.1 CO_2 adsorption studies by TPD

CO_2 adsorption capacities determined by TPD were obtained using a TPR/TPD, Quantachrome ChemBET model according to Moura and Pastore, 2013. Approximately 100 mg of the solids were placed in the reactor and treated for dehydratation at 225 °C, and then were cooled to the optimum adsorption temperatures previously determinated, at a cooling rate of 10 °C min^{-1} under He (30 mL min^{-1}). Then, the samples were held in this temperature for 2 h under CO_2/He (20 mL min^{-1}). The CO_2 was replaced by He (20 mL min^{-1}) and the sample was cooled to room temperature and held for 1 h to remove CO_2 adsorbed in solids. Finally, the desorption process started: the sample was heated from room temperature to 150 °C at a heating rate of 10 °C min^{-1}, monitored by a thermal conductivity detector connected to the output of the reactor. The amount of the carbon dioxide desorbed was determined by an external titration method.

3. RESULTS AND DISCUSSION

3.1 CO_2 adsorption studies by TPD

The time of 2 h was determinated as the optimal adsorption time due to the previously studied adsorption times. The results, not shown here, presented an increase of the adsorption capacity from 1 to 2 h but, decreased when the adsorption time increase to 3 or 5 h, indicating that the adsorption process does not suffer from kinetic limitations (Berkemeier *et al.*, 2013). Figures 1-3 displays the CO_2-TPD profile of all materials obtained in this work. The curves were decomposed using PeakFit deconvolution software, version 4.00.

For the N1-modified solid (Figures 1A and B) one peak at 146 and 149 °C or two peaks at about 127-136 and 147-150 °C could be observed. With longer pending groups, three peaks appear at 96-104, 120-133 and 149-150 °C. It is observed in Figures 1A (d) and 1B (d) that the profile of the TPD for 100% N1 shows only one peak. Considering that the ^{29}Si-NMR indicated that only T-sites are present in this material (Ferreira et *al*., 2008; Moura and Pastore, 2014), the desorption peak observed corresponds to the decomposition of the product of R-NH_2 pending groups with CO_2, that is, the propylammonium propylcarbamate, Figure 4a. However, in lower proportions of N1, free hydroxyl groups exist in the lamella, which allow formation of other compounds, such as hydrogen-bonded propylcarbamic acids or silylpropylcarbamates, Figure 4b e 4c (Danon *et al*., 2011). Since the last compound is more stable (Bacsik *et al*., 2011), in the other proportions of N1, silylpropylcarbamates and alkylammonium carbamate are formed during the CO_2 adsorption process and released at 127-136 °C and 146-150 °C, respectively, showing, contrary to the literature (Bacsik *et*

al., 2011), that alkylammonium alkylcarbamate ion pairs are released at a higher temperature than silylpropylcarbamates.

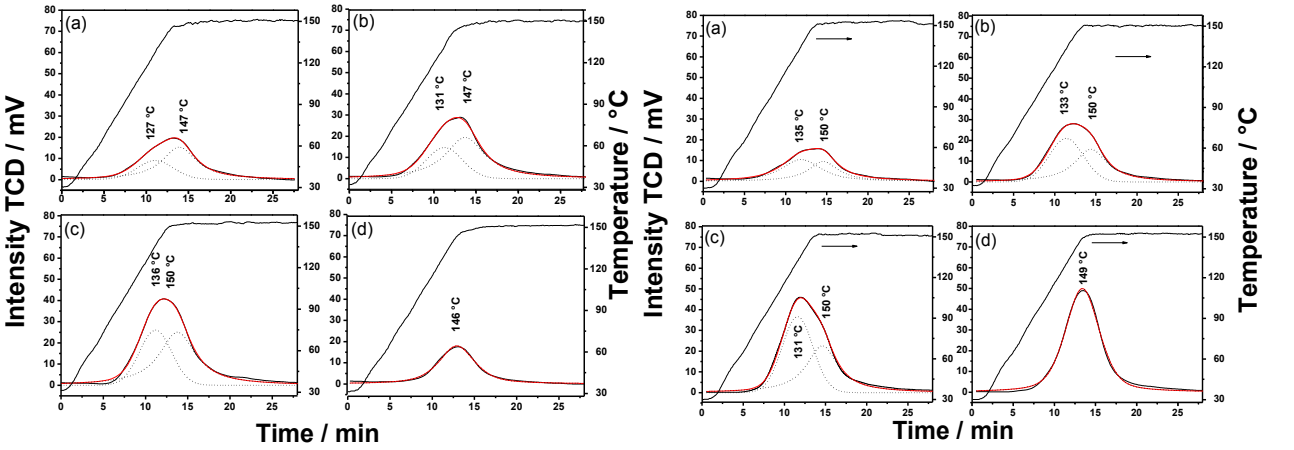

(A) (B)

Figure 1. Profile of temperature programmed desorption of CO_2 by organomagnesium phyllosilicates functionalized with N1 by conventional (A) and microwave oven (B).

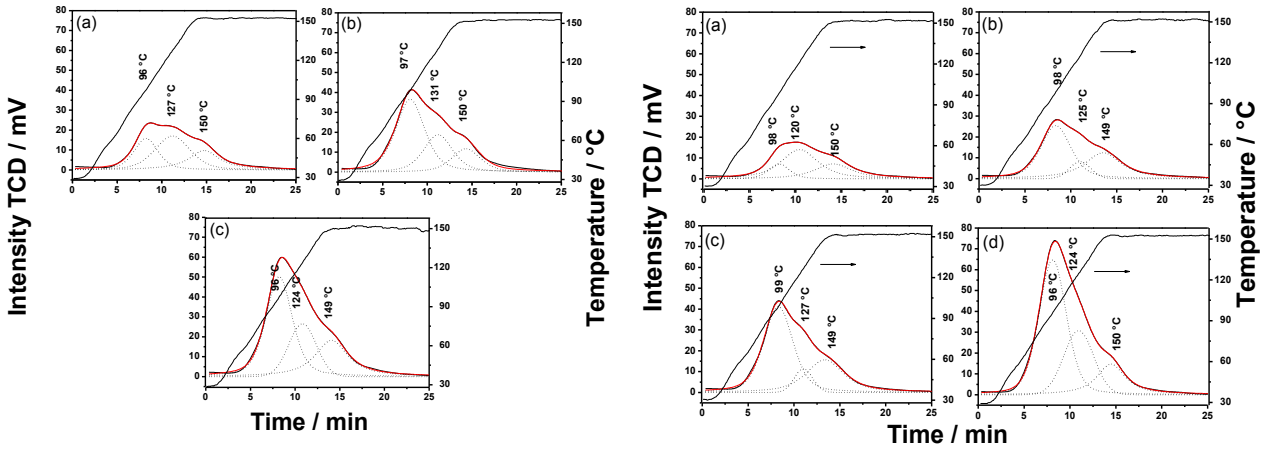

(A) (B)

Figure 2. Profile of temperature programmed desorption of CO_2 by organomagnesium phyllosilicates functionalized with N2 by conventional (A) and microwave oven (B).

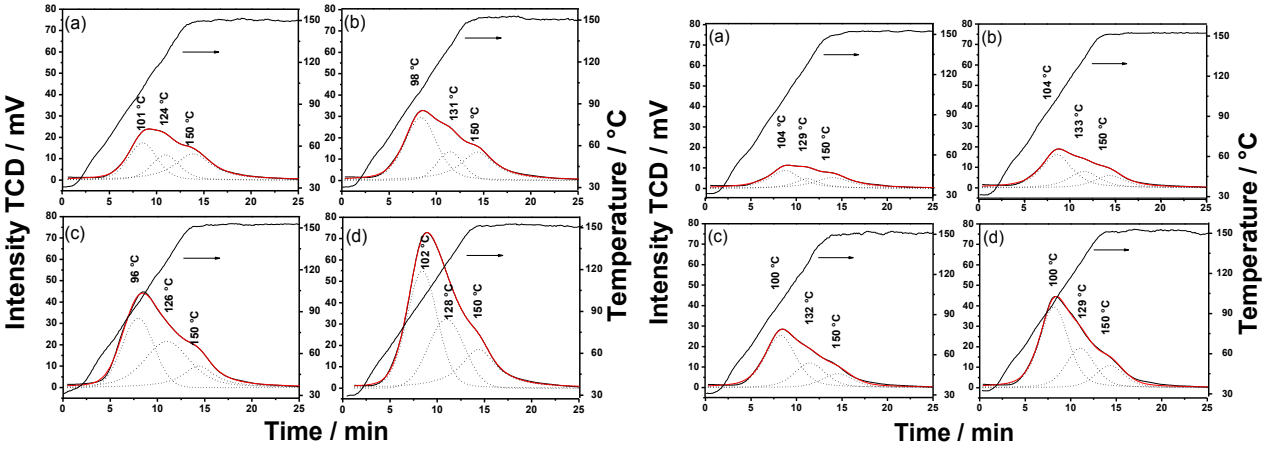

(A) (B)

Figure 3. Profile of temperature programmed desorption of CO_2 by organomagnesium phyllosilicates functionalized with N3 by conventional (A) and microwave oven (B).

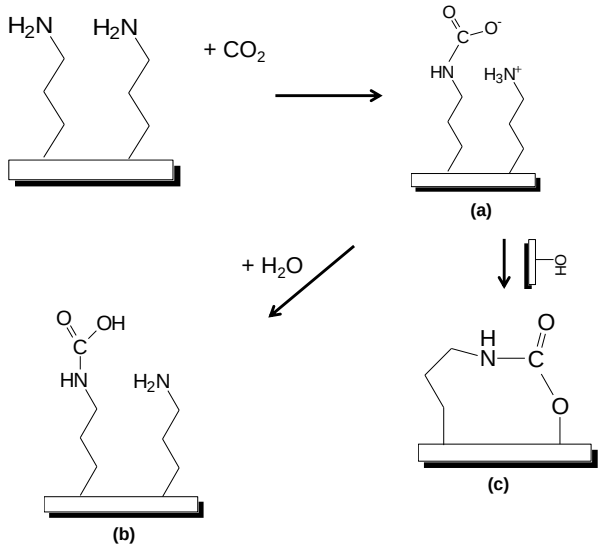

Figure 4: Adsorbed species on solid surfaces by the interaction between supported amines and CO_2: alkylammonium alkylcarbamate (a), hydrogen-bonded propylcarbamic acids (b), and silylpropylcarbamates (c).

Integration of the CO_2-TPD profiles, obtained using the Origin Software, version 8.0, provides curves, not shown here, allowing to obtain the maximum capacity (C_{max}) of materials, Table 1. C_{max} of materials prepared by conventional heating are higher than the ones prepared by microwave heating, except for 75% and 100% N1, and increase with the increased concentration of the alkylamine groups in the lamella of these materials. In these cases the concentrations of N found in the samples obtained by conventional heating are from 18 to 25% lower in relation the ones prepared using microwave heating, leading to a lower adsorption capacity. Smaller N concentrations were also found for 25 and 50% N1 and 25% N2 but the values are very close to the ones for samples prepared by microwave heating.

Table 1. Adsorption capacity and efficiency of the materials.

Molar Proportions / %	Conventional Heating			Microwave Heating		
	C_{max}*	N**	Eff***	C_{max}*	N**	Eff***
25 N1 – 75 TEOS	0.91	1.23	0.74	0.85	1.29	0.66
50 N1 – 50 TEOS	1.60	1.99	0.81	1.41	2.16	0.65
75 N1 – 25 TEOS	2.29	2.56	0.89	2.38	3.43	0.70
100 N1	0.89	3.14	0.28	2.02	3.84	0.62
12.5 N2 – 87.5 TEOS	1.47	1.90	0.78	0.98	1.49	0.66
25.0 N2 – 75.0 TEOS	2.03	2.51	0.81	1.22	2.60	0.47
37.5 N2 – 62.5 TEOS	2.84	3.37	0.84	2.09	3.02	0.69
50.0 N2 – 50.0 TEOS	[a]	[a]	[a]	3.23	4.03	0.80
8.33 N3 – 91.67 TEOS	1.41	1.67	0.84	0.67	1.16	0.58
16.67 N3 – 83.33 TEOS	1.59	2.57	0.62	0.97	2.09	0.47
25.00 N3 – 75.00 TEOS	2.32	3.24	0.72	1.32	2.61	0.50
33.33 N3 – 66.67 TEOS	3.64	4.05	0.90	2.05	3.76	0.54

* mmol CO_2 g^{-1}; ** mmol; *** mol CO_2 mol^{-1} N; [a] sample not obtained.

The C_{max} of CO_2 adsorption were in the range of 0.67 to 3.64 mmol CO_2 g^{-1}, corresponding to materials with Si_T/Si_{total} molar ratios of 8.33% N3, by microwave, and 33,33% N3, by conventional oven. Considering the efficiency of adsorption (Eff) of the materials, defined as the number of moles of carbon dioxide captured per number of moles of nitrogen in the interlayer space (Ko *et al*., 2011), the results obtained are in the range of 0.28 to 0.90, for amine/total Si molar ratios of 100% N1 and 33.33% N3, by conventional heating.

The Eff of the materials prepared by conventional heating is higher than the ones obtained using microwave as heating source, except for 100% N1, and, in the most of these results, the alkylamine efficiency found is higher than the maximum alkylamine efficiency, which is CO_2/N molar ratio of 0.5

under dry condition. This occurs, probably, because besides alkylammonium carbamate, other compounds, that do not involve a binary alkylaminic system, are also formed, allowing to obtain an amine efficiency higher than 0.5; this seems more meaningful for the materials obtained by conventional heating. In the case of 100% N1, the adsorption efficiency found for materials obtained by conventional heating is much lower than the one measured for the sample obtained by microwave probably because of the larger presence of alkylamine groups on the solid surface that can cause the interaction between neighbors alkylamine groups, thus reducing the adsorption sites.

The adsorption efficiencies of the materials prepared here are higher than the ones found in the literature: in the range (0.41-0.48), (0.15-0.24) and (0.12-0.29) mol CO_2 mol^{-1} N, for N1, N2 and N3, respectively (Wang *et al*., 2012); of 0.15, 0.21 and 0.10 for CO_2 on N1 functionalized MCM-41, SBA-15 and large pore SBA-15, respectively (Chang *et al*., 2009); of 0.24 for CO_2 adsorbed on N2 functionalized SBA-16 (Wei *et al*., 2008); of 0.336 for CO_2 adsorbed on N3 functionalized MS (mesoporous silica) (Kim *et al*., 2008); and, between 0.31 and 0.95, close to this work, were found using zeolite ITQ-6 functionalized with N1 (Zukal *et al.*, 2009).

Fast adsorption/desorption kinetics is one of the desired features for a good adsorbent. To evaluate desorption kinetics, the Avrami's exponential function, a case of the kinetic thermal decomposition model, was used. According to the literature, (Serna-Guerrero and Sayari, 2010; Kinefuchi *et al*. 2010; Stevens *et al.*, 2013), Equation 1 describes the general Avrami's model.

$$Q_t = Q^{max}(1 - exp(-(k_{av}t)^n)) \quad \text{(Eq. 1)}$$

In Eq. 1 k_{av} is the Avrami kinetic rate constant of CO_2 desorption, in min^{-1}, t is the reaction time, in min, n is the Avrami exponent (dimensionless), which is related to the CO_2 desorption order and to the changes of interaction mechanism, Q_t is the amount of CO_2 release at time t, and Q^{max} is the maximum amount of CO_2 released.

To determine the validity of the Avrami kinetic model and to ensure the reliability of the calculated parameters and validate their applicability, the function based on the normalized standard deviation (Eq. 2) was calculated.

$$SD(\%) = \sqrt{\frac{\Sigma\left[\left(Q_{t_{exp.}} - Q_{t_{mod.}}\right)/Q_{t_{exp.}}\right]^2}{n-1}}\ x100 \quad \text{(Eq. 2)}$$

In Eq. 2 $SD(\%)$ is the standard deviation function, $Q_{t_{exp.}}$ is the experimental data of the amount of CO_2 desorbed at time t, $Q_{t_{mod.}}$ is the amount desorbed as calculated by the Avrami model and n is the total number of the experimental points.

Table 2 shows the values of the kinetic parameters, along with the associated SD. The reaction order calculated by this model for the majority of the samples is in the range from 1.94 to 2.27, that is essentially 2, and 2.93 for 100% N1, and do not seem to display any relationship with the amount, or type, of the alkylamine used. Exception is made for the CO_2 desorption from 8.33% and 16.67% N3, by microwave, and 100% N1 by conventional heating: in these cases a fractional order was observed. According with the literature, the fractional order of this model arises, probably, from the complexity of the reaction mechanism, the occurrence of more than one reaction pathway during the desorption process (Serna-Guerrero and Sayari, 2010) or change of mechanisms during the desorption. In these particular cases, it may be also due to the type of species formed in the solid surface. The 7th column of Table 1 shows that the adsorption efficiencies from 8.33% and 16.67% N3, by microwave are the closest to 0.5, which is the case where the adsorption reaction probably favors the alkylammonium carbamate. The formation of other products in these materials is of lower importance. This observation suggests that in desorption, the order of the reaction, taken as the number of

different desorption mechanisms, would be the smallest. Attention is also drawn to 25.0% N2, 25% and 33.33% N3: the efficiencies are the same as 16.67% N3, but the reaction orders are next to 2. In these cases other factors, probably different mechanisms play a major role.

According to literature, the Avrami's exponent also depends on the nucleation rate and on the dimension of growth (Xie and Gao, 1998) of voids, since the decomposition process involves growing voids (Kinefuchi *et al.*, 2008) due to the release of the adsorption sites of CO_2. Considering the results found in this work, and according to Kinefuchi *et al.* 2008, when n values are between 2 and 3, the transformation is bidimensional. For n = 3 the nucleation rate is so low that the number of voids increases in a linear form in the time scale of the decomposition process.

The values of the k_{av} are in the range from 0.13 to 0.18 min^{-1}; these are overall constants representing various reaction steps described by the nonunitary order (n) obtained (Serna-Guerrero and Sayari, 2010). The results are similar to the literature: k_{av} in the range from 0.0232 to 0.2897 min^{-1} for CO_2 adsorbed on monoethanolamine functionalized TiO_2 (Sun *et al.*, 2011) and 0.0149 to 0.1644 min^{-1} for CO_2 desorption from Li_4SiO_4 (Qi *et al.*, 2013). The calculated standard deviations between the experimental and modeled values are within an acceptable degree of accuracy (Serna-Guerrero and Sayari, 2010).

Table 2. Values of the kinetic model parameters for CO_2 desorption.

Molar Proportions / %	Kinetics parameters					
	Conventional heating			Microwave heating		
	k_{av} /min^{-1}	*n*	SD (%)	k_{av} /min^{-1}	*n*	SD (%)
25 AMPTS – 75 TEOS	0.16	2.26	6.54	0.14	2.14	4.74
50 AMPTS – 50 TEOS	0.14	2.12	5.76	0.15	2.11	4.47
75 AMPTS – 25 TEOS	0.14	2.06	5.11	0.15	2.19	3.82
100 AMPTS	0.16	2.42	7.04	0.15	2.93	4.31
12.5 TMSPEDA – 87.5 TEOS	0.14	1.94	3.40	0.15	1.98	3.27
25.0 TMSPEDA – 75.0 TEOS	0.16	2.02	2.86	0.17	1.97	4.07
37.5 TMSPEDA – 62.5 TEOS	0.16	2.03	5.68	0.16	2.03	4.75
50.0 TMSPEDA – 50.0 TEOS	[a]	[a]	[a]	0.17	2.12	6.67
8.33 TMSPETA – 91.67 TEOS	0.14	2.02	6.15	0.14	1.72	3.18
16.67 TMSPETA – 83.33 TEOS	0.16	1.99	4.31	0.16	1.87	3.97
25.00 TMSPETA – 75.00 TEOS	0.13	2.27	3.32	0.18	1.95	4.41
33.33 TMSPETA – 66.67 TEOS	0.15	2.14	7.26	0.18	2.00	3.56

[a] sample not obtained.

4. CONCLUSION

The data presented in this work indicate that organofunctionalized magnesium phyllosilicates are promising adsorbents for CO_2. TPD technique shows that CO_2 adsorption capacity increase with the increased of the concentration of the pending groups in the interlayer space but, due to the diffusional difficulties, this capacity is reduced when 100% of the silicon atoms of the structure bear pending groups. The values corresponding to maximum efficiency of all the materials used as adsorbents are in the range of the 0.28 to 0.9 and, in most of these cases, were higher than 0.5, because other compounds are also formed besides alkylammomium carbamate, such as silylpropylcarbamates and hydrogen-bonded propylcarbamic acids. The materials prepared by conventional heating showed higher adsorption efficiency than the ones obtained

using microwave as heating source, except for 100% N1. Desorption kinetics of CO_2 was described successfully using Avrami's model. The CO_2 desorption rate constants are in the range from 0.13 to 0.18 min^{-1}. The reaction order calculated by this model was basically 2, or 3, except when 8.33% and 16.67% N3 obtained by microwave, and 100% N1 obtained by conventional heating, where a fractional order was observed probably due to the complexity of the reaction mechanism involved during the desorption process.

5. ACKNOWLEDGEMENTS

We are indebted to PETROBRAS for the financial support and K.O.M. for the fellowship. H.O.P. acknowledges Conselho Nacional de Desenvolvimento Científico e Tecnológico (CNPq) for the fellowship.

6. REFERENCE

BACSIK, Z.; AHLSTEN, N.; ZIADI, A.; ZHAO, G.; GARCIA-BENNETT, A. E.; MARTÍN-MATUTE, B.; HEDIN, N. Mechanisms and Kinetics for Sorption of CO_2 on Bicontinuous Mesoporous Silica Modified with n-Propylamine. **Langmuir** v. *27*, p. 11118–11128, 2011.

BERKEMEIER, T.; HUISMAN, A. J.; AMMANN, M.; SHIRAIWA, M.; KOOP, T.; POSCHL, U. Kinetic regimes and limiting cases of gas uptake and heterogeneous reactions in atmospheric aerosols and clouds: a general classification scheme. **Atmos. Chem. Phys.** v. 13, p. 6663–6686, 2013.

CHANDRASEKARAN, G.; HAN, H.-K.; KIM, G.-J.; SHIN, H.-J. Antimicrobial activity of delaminated aminopropyl functionalized magnesium phyllosilicates. **Appl. Clay Sci.** v. *53*, p. 729–736, 2011.

CHANG, F.-Y.; CHAO, K.-J.; CHENG, H.-H.; TAN, C.-S. Adsorption of CO_2 onto amine-grafted mesoporous silicas. **Sep. Purif. Technol.** v. *70*, p. 87–95, 2009.

DANON, A.; STAIR, P. C.; WEITZ, E. FTIR study of CO_2 adsorption on amine-grafted SBA-15: Elucidation of adsorbed species. **J. Phys. Chem. Chem. C.** v. 115, p. 11540−11549, 2011.

FERREIRA, R. B.; DA SILVA, C. R.; PASTORE, H. O. Aminopropyl-modified magnesium-phyllosilicates: layered solids with tailored interlayer access and reactivity. **Langmuir** v. *24*, p. 14215–14221, 2008.

JADHAV, P. D.; CHATTI, R. V.; BINIWALE, R. B.; LABHSETWAR, N. K.; DEVOTTA, S.; RAYALU, S. S. Monoethanol Amine Modified Zeolite 13X for CO_2 Adsorption at Different Temperatures. **Energy & Fuels**. v. 21, p. 3555–3559, 2007

KIM, S.-N.; SON, W.-J.; CHOI, J.-S.; AHN, W.-S. CO_2 adsorption using amine-functionalized mesoporous silica prepared via anionic surfactant-mediated synthesis. **Microporous Mesoporous Mater.** v. *115*, p. 497–503, 2008.

KINEFUCHI, I.; YAMAGUCHI, H.; SAKIYAMA, Y. TAKAGI, S.; MATSUMOTO, Y. Inhomogeneous decomposition of ultrathin oxide films on Si(100): application of Avrami kinetics to thermal desorption spectra. **J. Chem. Phys.** v. 128, p. 164712-164716, 2008.

KO, Y. G.; SHIN, S. S.; CHOI, U. S. Primary, secondary, and tertiary amines for CO_2 capture: designing for mesoporous CO_2 adsorbents. **J. Colloid Interf. Sci.** v. *361*, p. 594–602, 2011.

LAGADIC, I. L.; MITCHELL, M. K.; PAYNE, B. D. Highly effective adsorption of heavy metal ions by a thiol-functionalized magnesium phyllosilicate clay. **Environ. Sci. Technol.** v. *35*, 984–90, 2001.

LEE, Y.-C.; KIM, E. J.; YANG, J.-W.; SHIN, H.-J. Removal of malachite green by adsorption and precipitation using aminopropyl functionalized magnesium

phyllosilicate. **J. Hazard. Mater.** v. *192*, 62–70, 2011.

MOURA, K. O.; PASTORE, H. O. Comparative adsorption of CO_2 by mono-, di- and triamino- organofunctionalized magnesium phyllosilicates, **Environ. Sci. Technol.** v. 47, p. 12201-12210, 2013.

MOURA, K. O.; PASTORE, H. O. Physico-chemical characteristics of organo-functionalized magnesium phyllosilicate prepared by microwave heating. **Microporous Mesoporous Mater.**, 2014, DOI: 10.1016/j.micromeso.2014.02.027.

MOURA, H. M.; PASTORE, H. O. Functionalized Mesoporous Solids Based on Magadiite and [Al]-Magadiite. **Dalton Transactions**, 2014, DOI: 10.1039/C3DT53571A.

PATEL, H. A.; SHARMA, S. K.; JASRA, R. V. Synthetic talc as a solid base catalyst for condensation of aldehydes and ketones. **J. Mol. Catal. A: Chem.** v. *286*, 31–40, 2008.

PLAZA, M. G; PEVIDA, C.; ARENILLAS, A.; RUBIERA, F.; PIS, J. J. CO_2 capture by adsorption with nitrogen enriched carbons. **Fuel.** v. 86, p. 2204–2212, 2007.

QI, Z.; DAYING, H.; YANG, L.; QIAN, Y.; ZIBIN, Z. Analysis of CO_2 sorption/desorption kinetic behaviors and reaction mechanisms on Li_4SiO_4. **AIChE J.** v. 59, p. 901−911, 2013.

SAMANTA, A.; ZHAO, A.; SHIMIZU, G. K. H.; SARKAR, P.; GUPTA, R. Post-Combustion CO_2 Capture Using Solid Sorbents : A Review. **Ind. Eng. Chem. Res.** v. *51*, p. 1438–1463, 2012.

SAYARI, A.; BELMABKHOUT, Y.; SERNA-GUERRERO, R. Flue gas treatment via CO_2 adsorption. **Chem. Eng. J.** v. *171*, p. 760–774, 2011.

SERNA-GUERRERO, R.; SAYARI, A. Modeling adsorption of CO_2 on amine-functionalized mesoporous silica. 2: Kinetics and breakthrough curves. **Chem. Eng. J.** v. *161*, p. 182–190, 2010.

SHAFEEYAN, M. S.; DAUD, W. M. A. W.; HOUSHMAND, A.; SHAMIRI, A. A review on surface modification of activated carbon for carbon dioxide adsorption. **J. Anal. Appl. Pyrol.** v. *89*, p. 143–151, 2010.

STEVENS, L.; WILLIAMS, K.; HAN, W. Y.; DRAGE, T.; SNAPE, C.; WOOD, J.; WANG, J. Preparation and CO_2 adsorption of diamine modified montmorillonite via exfoliation grafting route. **Chem. Eng. J.** v. 215−216, p. 699−708, 2013.

VIEIRA, R. B.; PASTORE, H. O. Polyethylenimine-Magadiite Layered Silicate Sorbent for CO_2 Capture. **Environ. Sci. Technol.** DOI 10.1021/es404501e.

SUN, Z.; FAN, M.; ARGYLE, M. Desorption kinetics of the monoethanolamine/ macroporous TiO_2-based CO_2 separation process. **Energy Fuels** v. 25, p. 2988−2996, 2011.

WANG, J.; STEVENS, L. A.; DRAGE, T. C.; WOOD, J. Preparation and CO_2 adsorption of amine modified Mg–Al LDH via exfoliation route. **Chem. Eng. Sci.** v. *68*, p. 424–431, 2012.

WEI, J.; SHI, J.; PAN, H.; ZHAO, W.; YE, Q.; SHI, Y. Adsorption of carbon dioxide on organically functionalized SBA-16. **Microporous Mesoporous Mater.** v. *116*, p. 394–399.

XIE, X.; GAO, H. Calorimetric studies on the crystallization of Li_2S-B_2O_3 glasses. **J. Non-crystalline Solids.** v. 240, p. 166-167, 1998.

ZUKAL, A.; DOMINGUEZ, I.; MAYEROVÁ, J.; CEJKA, J. Functionalization of delaminated zeolite ITQ-6 for the adsorption of carbon dioxide. **Langmuir**. v. *25*, p. 10314–10321, 2009.